DESIGN OF BUBBLE COLUMNS EQUIPPED WITH POROUS SPARGER

A.A. Mouza

Chemical Process and Plant Design Laboratory

Chemical Engineering Department, Aristotle University of Thessaloniki, Greece

mouza@auth.gr

ABSTRACT

Bubble columns are widely used in industrial gas-liquid operations (e.g. gas/liquid reactions, agitation by gas injection, fermentations etc.) in chemical and biochemical process industries, due to their simple construction, low operating cost and high energy efficiency. In all these processes gas holdup and bubble size are important design parameters, since they define the gas-liquid interfacial area available for mass transfer. In turn, bubble size distribution and gas holdup depend largely on column geometry, operating conditions, physico-chemical properties of the two phases and type of gas sparger. This work concerns the effect of liquid phase properties on the performance of bubble column equipped with metal porous sparger. Based on experimental data obtained using several Newtonian and non-Newtonian liquids generalized correlations are formulated, which can predict with reasonable accuracy the transition point from homogenous to heterogeneous regime as well as the gas hold up and the mean bubble size at the homogenous regime.

INTRODUCTION

Bubble columns are widely employed gas-liquid contactors (***Figure 1***). Their use covers chemical, petrochemical, bioprocessing, bioremediation applications. Compared to other types of reactors their main advantages are the absence of moving parts (resulting in lower energy consumption), the high heat and mass transfer rates and the ease of long-term sterile operation. Bubble columns are also essential in the cultivation of shear sensitive cultures (e.g. microbial fermentations, fragile biocatalysts, and animal and plant cell cultures), due to the controllable shear rates applied inside the column. Several bubble column applications also involve non-Newtonian shear thinning liquids (e.g. polymer solutions, gels, slurries, foams etc.), whose viscosity greatly depends on the shear rate generated inside the column by the ascending bubbles.

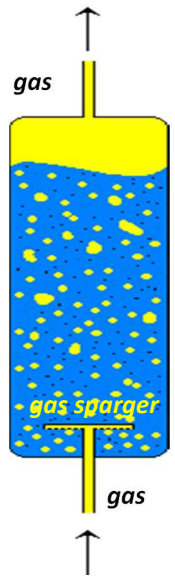

***Figure 1**. Typical bubble column*

Depending on the gas flow rate two main flow regimes are observed in bubble columns, namely the ***homogeneous regime*** and the ***heterogeneous*** regime. The homogenous regime, encountered at low gas velocities and characterized by discrete and relatively small bubbles, is usually the most desirable because it enhances the efficiency of the equipment by providing a greater gas-liquid interfacial area. The ***heterogeneous*** (churn-turbulent flow) ***regime*** is observed at higher gas velocities and characterized by the appearance of large bubbles that ascend with higher velocity and lead to lower gas holdup values.

In bubble column applications the mass transfer rate depends on the gas/liquid interfacial area (***α***), which is a function of the gas holdup (***ε_G***) and the mean Sauter diameter (***d_{32}***) of the bubbles (***Eq.1***):

$$a = \frac{6\varepsilon_G}{d_{32}} \tag{1}$$

In turn, the values of ***ε_G*** and ***d_{32}***, which are known to be mainly controlled by phenomena (i.e. bubble coalescence and/or breakage) occurring onto or in the vicinity of the sparger, depend on the geometry of the column, the operating conditions, the physicochemical properties of the two phases and

the type of gas sparger. Among the various types of gas spargers employed, ***porous spargers*** are known to produce more numerous and smaller bubbles.

As the multiphase flow is in general complex in structure, the design of bubble columns is primarily carried out by means of empirical or semi-empirical correlations based mainly on experimental data. The work conducted in our Lab during the last decade concerns bubble columns equipped with fine pore metal spargers and has led to the development of design equations that can predict with reasonable accuracy the gas holdup and the mean Sauter diameter at the homogenous regime as well as the transition point from homogenous to heterogeneous regime [1-7]. The validity of the proposed correlations has been checked with data obtained using different geometrical configurations as well as various Newtonian and non-Newtonian liquids.

EXPERIMENTAL SET-UP AND PROCEDURES

The experimental set-up (***Figure 2***) consists of a vertical Plexiglas® cylindrical column equipped with a 316L SS porous disk (Mott Corp.) sparger with nominal pore size of 40 μm or 100 μm. The sparger is located at the center of the bottom column plate and may cover either part of or the entire cross section. To eliminate image distortion caused by refraction due to the cylindrical column wall, the column is placed into a square cross-section Plexiglas® box filled with the fluid used for the corresponding experiment.

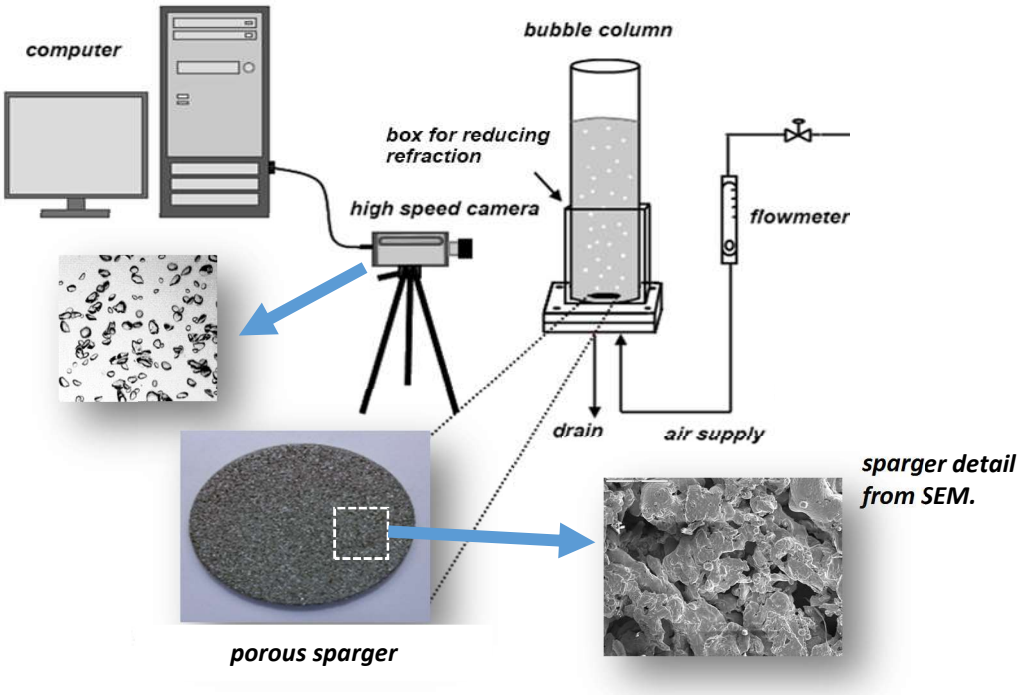

Figure 2. *Experimental set up.*

To ensure that, especially for the lower gas flow rates employed, the gas phase is equally distributed over the sparger area, several gas entrance configurations were proposed and their efficiency, both in terms of gas distribution uniformity and ease of construction, was evaluated by performing appropriate *CFD* simulations[6]. The simulation results lead to the adoption of the design presented in ***Figure 3***, i.e. the injection of the gas phase through a 1 cm nozzle to a vessel of 35 cm height placed beneath the bubble column. The corresponding experiments confirmed that the bubbles are evenly created over the entire sparger surface.

All the experiments were performed at atmospheric pressure and ambient temperature conditions (25±1 ºC). The viscosity of the Newtonian fluids was measured by a KPG Cannon–Fenske (Schott®)

viscometer, while that of the non-Newtonian fluids using a Magnetic Bearing rheometer (AR-G2 TA Instruments®). The surface tension of all liquids was determined by the pendant drop method (KSV® CAM 200). The liquid phase was water as well as aqueous glycerin and aqueous butanol solutions, which cover a density range of 998-1180 kg/m^3, a viscosity range of 0.9-20 mPas and have surface tension values of 48-72 mN/m [1,2,3]. With the addition of small amounts of various surfactants, namely *Triton, CTAB* and *SDS*, the surface tension of the above liquids becomes 31-59 mN/m [2]. To render the solutions non-Newtonian a small amount of xanthan gum (~0.35mg/L) is added to the aforementioned solutions [5,6,7]. The gas phase used was dry compressed air.

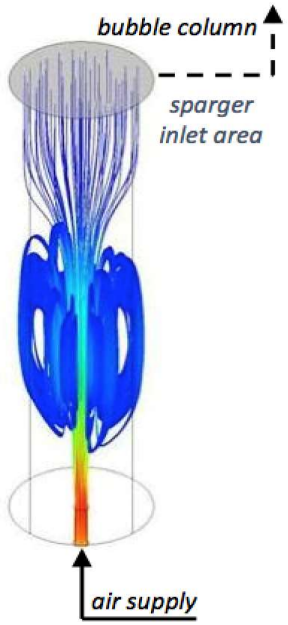

***Figure 3**. Gas entrance section*

All the experiments were performed with no liquid throughput. Each run starts by filling the column with the liquid to a height appropriate to ensure that gas holdup measurements are independent of the liquid level. The test section is positioned between the camera and an appropriate lighting system placed behind a diffuser to evenly distribute the light. The average gas holdup is estimated by recording the liquid level ***before*** and ***after*** the gas injection (at steady state) by a video camera (*Redlake MotionScope PCI® 1000S*). The bed expansion is calculated by superimposing the relevant pictures using suitable software (*RedLake Imaging MotionScope® 2.30*). Finally, for each gas flow rate the gas holdup is calculated, with a maximum uncertainty of less than 15%, by averaging the liquid level differences at five consecutive instances covering a time length of 10 s.

The bubble size distribution is estimated by applying an appropriate software (*RedLake Imaging Motion Scope® 2.30*) on images of the bubbles acquired by the video camera. For each liquid, a statistically adequate number of 100 bubbles were measured at the vicinity of the sparger. The spatial resolution of the measuring technique is approximately 80 μm, while the maximum error is estimated to be less than 10%. The Sauter mean diameter (d_{32}) of the bubbles is calculated by:

$$d_{32} = \frac{\sum_i^N n_i d_{Bi}^3}{\sum_i^N n_i d_{Bi}^2} \qquad (2)$$

where d_{Bi} and n_i are the diameter and the number of the bubbles of size class *i* respectively and *N* is the number of classes used for the distribution.

RESULTS AND DISCUSSION

The experiments reveal that the design parameters, namely the transition point from homogenous to heterogeneous regime as well as the gas hold up and the Sauter mean bubble diameter at the homogenous regime, mainly depend on:

- the gas phase *superficial velocity*, defined as $U_{GS}=Q_G/A$, where Q_G is the gas flow rate and *A* the column cross section,
- the *physical properties* of the liquid phase, namely the density (ρ_L), the viscosity (μ_L) (***Figure 4***), and the surface tension (σ_L) (***Figure 5***),
- the type and concentration of the surfactant added (***Figure 6***),
- the column and the sparger diameter, d_C and d_S respectively and
- the mean porous diameter of the sparger, d_p.

By performing dimensional analysis generalised designing correlations appropriate for bubble columns with porous sparger have been formulated [1-7], the validity of which has been checked with relevant experimental data.

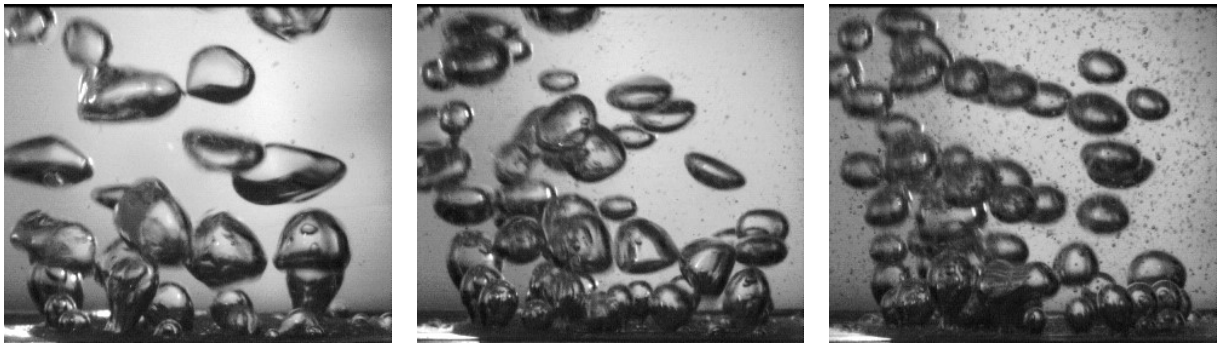

μ_L=1.0 mPa s μ_L=6.2 mPa s μ_L=16.6 mPa s

Figure 4.*Effect of liquid viscosity on bubble size Q_G=14.7 cm^3/s*

σ=72 mN/m σ=60 mN/m σ=50 mN/m

Figure 5. *Effect of surface tension on bubble size Q_G=18.5 cm^3/s.*

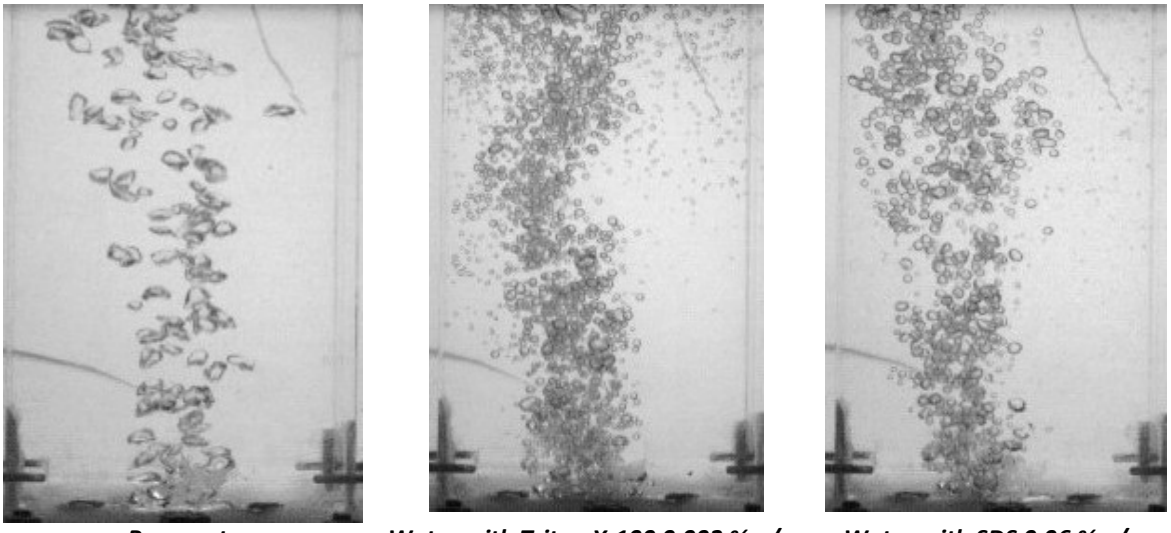

Pure water ***Water with Triton X-100 0.002 %w/w*** ***Water with SDS 0.06 %w/w***

Figure 6. *Effect of surfactant addition on bubble size for the same gas flow rate.*

In the case of the non-Newtonian fluids, since their viscosity is a function of the shear rate, an ***effective*** viscosity, μ_{eff}, is introduced, which corresponds to the volume averaged shear rate inside the column. In turn, the volume averaged shear rate is assessed by performing *CFD* simulations using

the commercial code *Ansys-CFX*. The code uses the *Multiple Size Group* (*MUSIG*) model for handling polydispersed multiphase flows, i.e., bubbles of various sizes. The ***initial bubble size distribution*** required as input is experimentally measured. The code is validated by comparing the experimental and calculated gas phase velocity fields. To accomplish this, we performed a qualitative reconstruction of the flow patterns in the bubble column by applying cross correlations algorithms on consecutive bubble images. The procedure followed for the flow field measurement is based on the well-known Particle Image Velocimetry (*PIV*) technique used in our Lab, which has been adapted for bubble velocity measurements [6]. The good agreement between numerical and experimental flow maps ***(Figure 7)***, confirms that *CFD* can quite accurately predict the flow pattern of the gas and consequently the shear rate distribution inside the column.

It is found that the dependence of a volume average shear rate, γ_m, on gas superficial velocity can be expressed with reasonable accuracy (±15%) by ***Eq. 3*** [6,7]:

$$\gamma_m = 70 \cdot U_{GS}^{0.48} \tag{3}$$

Using the predicted γ_m value, an ***effective*** viscosity, μ_{eff}, can be calculated.

During the period of the experiments the use of several porous discs with the same nominal porosity proved that the data are quite reproducible and that the porous disc usage time does not significantly affect its performance.

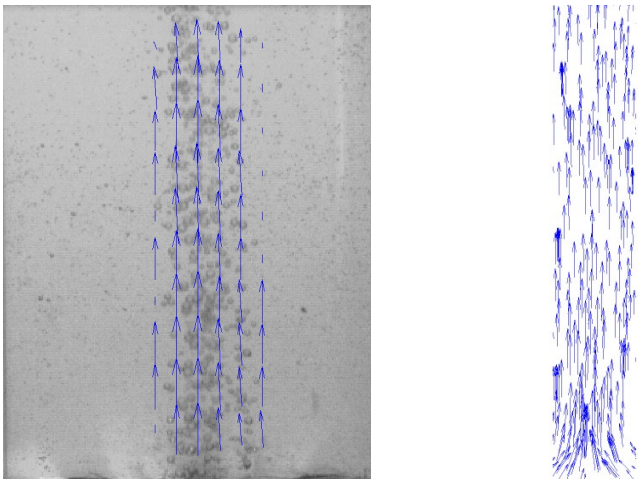

experimental ***numerical (CFD)***

Figure 7. *Comparison of experimental with numerical gas velocity fields for water (U_{GS}=0.002 m/s).*

Transition point to heterogeneous regime

The dimensional analysis reveal that the transition point between homogenous and heterogeneous regime can be predicted with an accuracy of *±10%* by ***Eq.3***: [2,7]:

$$Fr_{trans} = a_1 \left[Eo^{a_2} \left(\frac{d_s}{d_c} \right)^{a_3} \right]^{a_4} \tag{4}$$

where Fr_{trans}, is the *Froude* number based on the velocity at the transition point and *Eo*, the *Eötvös* number defined as:

$$Fr_{trans} = \frac{U_{GS,trans}^2}{d_p g} \tag{5}$$

$$Eo = \frac{d_C^2 \rho_L g}{\sigma_L} \tag{6}$$

with $U_{GS,trans}$ being the gas superficial velocity at the transition point, d_P the mean pore diameter of the porous sparger and d_C the column diameter. To incorporate the effect of different geometrical configurations of the gas entrance, the ratio of sparger to column diameter (d_S/d_C) is also included. The constants a_{1-4} depend on the type of fluid, i.e. Newtonian, non-Newtonian, addition of surfactants. ***Figure 8*** shows a typical comparison between ***Eq. 4*** and experimental data.

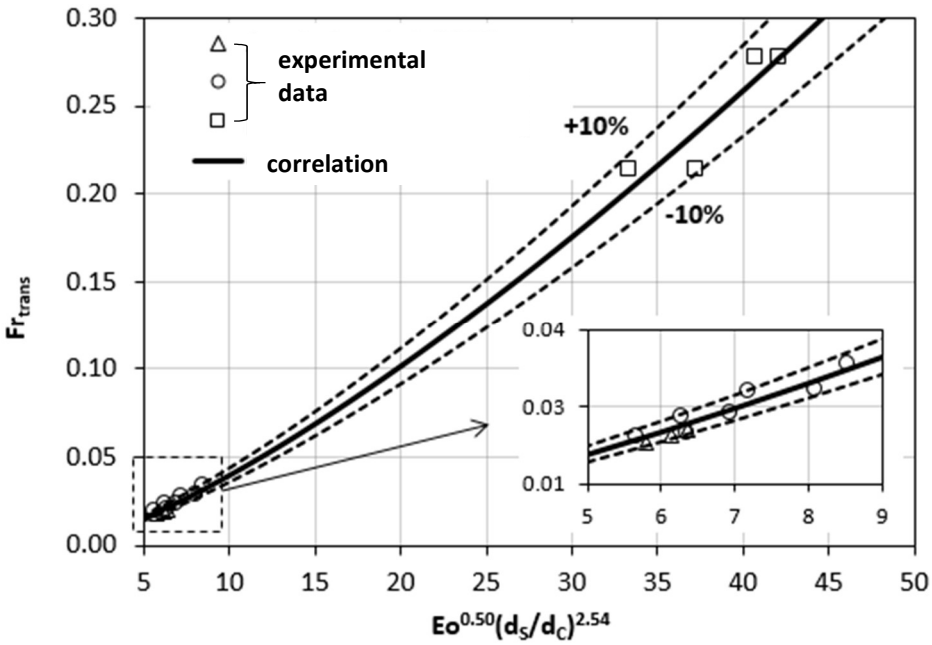

Figure 8. *Comparison of the regime transition prediction with experimental data (non-Newtonian fluids with surfactants).*

Prediction of bubble diameter

It is found that the *Sauter* mean diameter (d_{32}) of the bubbles at the homogenous regime can be predicted by ***Eq.6*** with an accuracy of ±15% (***Figure 9***) [3,7]:

$$\frac{d_{32}}{d_s} = b_1 \left[We^{b_2} \, \mathrm{Re}^{b_3} \, Fr^{b_4} \left(\frac{d_p}{d_s} \right)^{b_5} \right]^{b_6}$$

where the constants b_{1-6} depend on the type of fluid, *We* is the *Weber*, *Re* the *Reynolds* and *Fr* the *Froude* number respectively, defined as:

$$We = \frac{\rho_L U_{GS}^2 d_s}{\sigma_L} \tag{8}$$

$$\mathrm{Re} = \frac{\rho_L U_{GS} d_s}{\mu} \tag{9}$$

$$Fr = \frac{U_{GS}^2}{d_c g} \tag{10}$$

When the liquid phase is a non-Newtonian fluid the ***effective*** viscosity must be used.

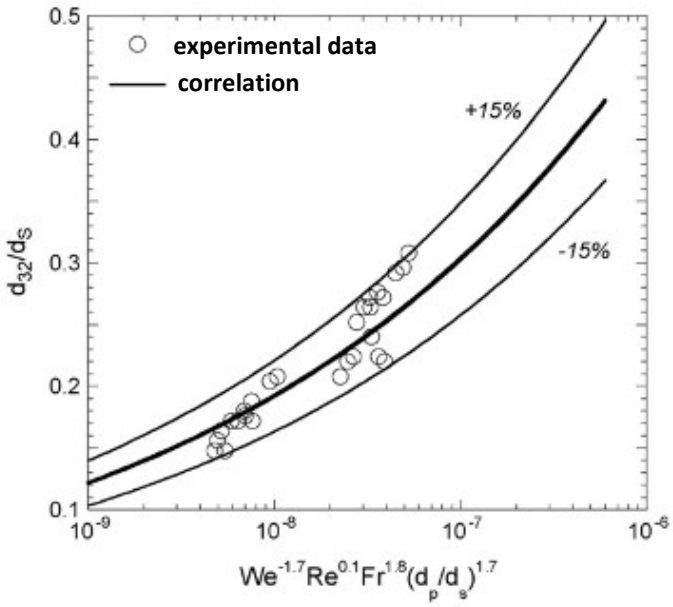

***Figure 9**. Prediction of d_{32}* for Newtonian liquids.

Prediction of gas holdup

The average gas hold-up value ε_g can be predicted with an accuracy of *±20%* by ***Eq.11*** [1,2,4-7]

$$\varepsilon_g = c_1 \left[Fr^{c_2} Ar^{c_3} Eo^{c_4} \left(\frac{d_s}{d_c}\right)^{c_5} \left(\frac{d_p}{d_s}\right)^{c_6} \right]^{c_7} \tag{11}$$

The constants $c_{1\text{-}7}$ depend on the type of liquid and *Ar* is the *Archimedes* number defined as:

$$Ar = \frac{d_C^{\,3} \rho_L^{\,2} g}{\mu_L^2} \tag{12}$$

The gas holdup values calculated by the proposed correlation are found to be in good agreement with experimental data obtained using various types of liquids ***(Figure 10***).

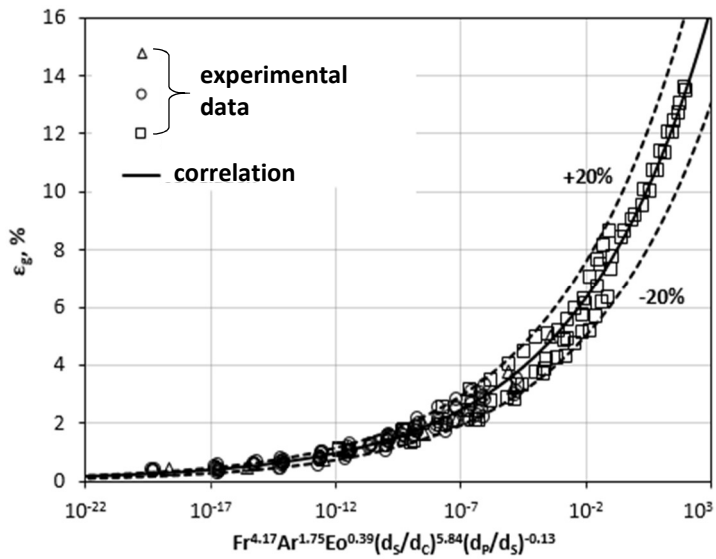

***Figure 10**. Comparison of gas holdup correlation with experimental data* (non-Newtonian liquids).

For the sake of conciseness the values of the constants involved in ***Eqs. 4, 6*** and ***11*** are not listed here but can be found in the relevant publications [1-7].

CONCLUSIONS

The main intention of the work conducted in our Lab was to better understand and interpret the phenomena that occur in the course of bubble formation in bubble columns. Based on our observations we were also able to develop correlations that incorporate dimensionless numbers and can be used for predicting the most important parameters for bubble column design. The proposed correlations provide the designer with a means of estimating quickly and with reasonable accuracy the regime transition point, the average gas holdup and the mean bubble size.

ACKNOWLEDGMENTS

I must acknowledge here the contribution of all my students from 2004 till now, namely G. Dalakoglou, I. Papadopoulos, N. Kazakis, A. Anastasiou, A. Passos, A. Koletti and V. Voulgaropoulos. I owe special thanks to our lab technicians A. Lekkas, F. Lampropoulos and T. Tsilipiras for their cooperation and their invaluable help in the construction of the various experimental set ups. I must also thank Prof. S.V. Paras for his valuable comments and suggestions.

REFERENCES

[1] Mouza, A.A., Dalakoglou, G.K., Paras, S.V. (2005). *Chem. Eng. Sci*., 60(5): 1465-1475.
[2] Kazakis, N.A., Papadopoulos, I.D., Mouza, A.A. (2007). *Chem. Eng. Sci*., 62: 3092-3103
[3] Kazakis, N.A., Mouza, A.A., Paras, S.V. (2008). *Chem. Eng. J.*, 137(2): 265-281.
[4] Anastasiou, A.D., Kazakis, N.A., Mouza, A.A., Paras, S.V. (2010). *Chem. Eng. Sci*., 65: 5872-5880.
[5] Anastasiou, A.D., Koletti, A.E., Mouza, A.A. (2011). *8th Nat. Chem. Eng. Conference*, Thessaloniki, Greece
[6] Anastasiou, A.D., Passos, A.D., Mouza, A.A. (2013). *Chem. Eng. Sci*., 98: 331-338.
[7] Passos, A.D., Voulgaropoulos, V.P., Paras, S.V., Mouza, A.A. (2015). *Chem. Eng. Res. Des.*, 95: 93-104.